

NUMERICAL STUDY OF THE NON-NEWTONIAN BLOOD FLOW IN A STENOSED ARTERY USING TWO RHEOLOGICAL MODELS

by

Louiza ACHAB*, Mohamed MAHFOUD, and Salah BENHADID

Theoretical and Applied Fluid Mechanics Laboratory, Sciences and Technology University,
USTHB, Algiers, Algeria

Original scientific paper
DOI:10.2298/TSCI130227161A

The numerical simulation of blood flow in arteries using non-Newtonian viscosity model, presents two major difficulties; the first one is the choice of an appropriate constitutive equation, because no one model is universally accepted as a reflection of the true behavior of blood viscosity until now. Another difficulty lies in the numerical convergence of the complex scheme solving the highly non-linear set of equations governing the blood motion. In this paper, the pulsatile blood flow through an arterial stenosis has been numerically modeled to evaluate the flow characteristics and the wall shear stress under physiological conditions. The Navier-Stokes equations governing the fluid motion are solved using the finite element method in unsteady 2-D case. The behavior of blood is considered as the generalized power-law and Cross models, where the shear-thinning characteristics of the streaming blood are taken into account. Constants in the constitutive equations of previous models have been obtained by fitting experimental viscosity data. The numerical simulations are performed for a wide range of apparent shear rates (10 s^{-1} - 750 s^{-1}) with good convergence of the iterative scheme. Results from the blood flow simulations indicate that non-Newtonian behavior has considerable effects on instantaneous flow patterns. However, it seems that the generalized power-law model will be slightly better for describing the non-Newtonian characteristics of blood than the Cross model.

Key words: *pulsatile blood flow, Generalized power-law, Cross law, stenosis, finite element method, Galerkin, penalty function*

Introduction

The study of the blood flow has attracted many researchers over the past years. Due to its significant effect on several human cardiovascular diseases, detailed knowledge of blood flow in physiological conditions is required. Among the various cardiovascular diseases, arteriosclerosis is a major one which affects the flow of blood through the arteries. This abnormality, frequently occurring in man, is characterized by progressive narrowing and hardening of artery over time. It results in its advanced stages, in lesions that protrude into the arterial lumen, leading ultimately to vessel stenosis and obstruction of blood flow. The problem of blood flow through stenosis has been reported by several investigators, under various conditions, to explore the relationship between various flow characteristics and early atherosclerotic lesion development. Extensive experimental and numerical approaches for steady flow through stenosis have been carried out, treating blood as a Newtonian fluid [1-3]. These stud-

* Corresponding author; e-mail: l_achab@yahoo.fr

ies mainly provided insights into the dependence of flow patterns on geometry and upstream Reynolds number. Pulsatile flow effects in stenotic geometries have also been numerically studied in the 2-D and 3-D cases [4-6], with the flow being considered as a Newtonian fluid. However, it has demonstrated that human blood behaves as a Newtonian fluid at large shear rates [7], and exhibits predominantly the behaviour of non-Newtonian fluid at low shear rates; particular, in some diseased conditions and in the pulsatile flow case, in which blood is subjected to cyclic low shear rates for a major part of the time period [8, 9].

In order to have a complete understanding of the flow through stenotic artery from the physical point of view, one needs to be fully conversant with the hemodynamic behaviour of blood together with its rheological properties. The mathematical study of meaningful constitutive models that can accurately capture the rheological response of blood, over a range of shear rate, is recognized as an invaluable tool for the interpretation and analysis of blood flow in physiological and pathological conditions. Several theories have proposed to describe the complex behaviour of the non-Newtonian fluid of blood, especially in unsteady flow, by using different blood viscosity models [10-15]. Details of a recent comparison between a Newtonian, Casson, Power-law, and Quemada model are to be found in the paper of Neofytou [16], in the case of channel flow where part of one of the channel walls was forced to oscillate laterally. The Casson and Quemada models were seen to agree well in their predictions and were preferred over the Power-law model. Tu and Deville [17] considered blood obeying the Hershell-Bulkley, Bingham and Power-law fluid models, through arterial stenosis. The models predictions were compared to those obtained with the Newtonian fluid law for both steady and pulsatile flow. Buchanan *et al.* [18] employed the Quemada and Power-law models in pulsatile laminar flow through an axisymmetric stenosed tube; they found that the rheological models could affect wall shear stress quantities. More recently, Modarres Razavi *et al.* [19] compared for the same rheological models with Newtonian one, the hemodynamic wall parameters in pulsatile nature of blood flow for various Womersley numbers, they concluded from their investigations that the non-Newtonian rheology of blood affects the flow field. These studies have all indicated the significant role of non-Newtonian behavior of blood in flow characteristic through stenotic artery. However, due to the complex chemical structure of the blood and the increased rate of collisions between aggregates, none of the constitutive equations studied so far seems to be completely satisfactory in all deformation ranges.

The purpose of this paper is to simulate the periodic flow through a stenotic artery by a finite element method, using penalty function approach, and to compare the effects of non-Newtonian blood viscosity model on flow patterns during the cardiac cycle. The blood is treated using the namely cross and Generalized power-law (GPL) constitutive equations. Our choice of the first model is dictated by capturing some of the physical properties of blood viscosity variation in medium and high shear rate and the second one, recently proposed in [20] is a generalization and combination of some classical models used for blood.

Numerical modeling

In this work, blood is modeled as an incompressible and isothermal fluid. The flow through the artery is laminar, axisymmetric, and fully developed. The governing equations, corresponding to the conservation of mass and momentum, can be written:

– continuity equation

$$\frac{\partial u}{\partial r} + \frac{u}{r} + \frac{\partial w}{\partial z} = 0 \quad (1)$$

– momentum equation

$$\rho \frac{\partial u}{\partial t} + \rho \left(u \frac{\partial u}{\partial r} + w \frac{\partial u}{\partial z} \right) = - \frac{\partial p}{\partial r} + \mu(\dot{\gamma}) \left(\frac{\partial \tau_{rr}}{\partial r} + \frac{\partial \tau_{zr}}{\partial z} + \frac{\tau_{rr} - \tau_{\theta\theta}}{r} \right) \quad (2)$$

$$\rho \frac{\partial w}{\partial t} + \rho \left(u \frac{\partial w}{\partial r} + w \frac{\partial w}{\partial z} \right) = - \frac{\partial p}{\partial z} + \mu(\dot{\gamma}) \left(\frac{\partial \tau_{zr}}{\partial r} + \frac{\partial \tau_{zz}}{\partial z} + \frac{\tau_{zr}}{r} \right) \quad (3)$$

For an axisymmetric flow, the components of the deviatoric stress tensor may be expressed:

$$\tau_{rr} = 2\mu(\dot{\gamma}) \left(\frac{\partial u}{\partial r} \right), \quad \tau_{zz} = 2\mu(\dot{\gamma}) \left(\frac{\partial w}{\partial z} \right), \quad \tau_{zr} = \mu(\dot{\gamma}) \left(\frac{\partial u}{\partial z} + \frac{\partial w}{\partial r} \right), \quad \tau_{\theta\theta} = 2\mu(\dot{\gamma}) \frac{u}{r}$$

The shear rate $\dot{\gamma}$, is obtained from the second invariant of the tensor such that:

$$\dot{\gamma} = \sqrt{2 \left[\left(\frac{\partial w}{\partial r} \right)^2 + \left(\frac{w}{r} \right)^2 + \left(\frac{\partial u}{\partial z} \right)^2 \right] + \left(\frac{\partial w}{\partial z} + \frac{\partial u}{\partial r} \right)^2} \quad (4)$$

In eqs. (1)-(4), u and w are the radial and the axial velocity components in the r - and z - directions, respectively, p – the pressure, t – the time, τ_{ij} – the stress tensor, ρ – the blood density, and $\mu(\dot{\gamma})$ – the non-Newtonian dynamical viscosity. Characteristic parameters of the blood flow include also, Reynolds number, and Womersley number, α , which can be defined, respectively:

$$\text{Re} = \frac{\rho w_{\max} D}{\mu_{\infty N}}, \quad \alpha = D \sqrt{\frac{2\pi f \rho}{\mu_{\infty N}}}$$

Here the Reynolds number is defined in terms of the maximum centreline velocity w_{\max} , the vessel diameter D , the density of the plasma and Newtonian limit viscosity of the flow under consideration. Also the Womersley number is function of the blood density, diameter artery, Newtonian limit viscosity, and pulsatile flow frequency, f .

The rheological properties of blood are modeled through the specification of a constitutive relation for dynamical viscosity, $\mu(\dot{\gamma})$. In this study, the only non-Newtonian effect that is taken into account is the shear-thinning behavior. The constitutive equation for the Cross law [21], based on the stress-strain rate relationship is given by:

$$\begin{cases} \tau = \mu(\dot{\gamma})\dot{\gamma} \\ \mu(\dot{\gamma}) = \mu_{\infty} + \frac{\mu_0 - \mu_{\infty}}{1 + (\beta\dot{\gamma})^p} \end{cases} \quad (5)$$

where $\dot{\gamma}$ is the local shear rate, μ_{∞} and μ_0 are the asymptotic apparent viscosities as $\dot{\gamma}$ tends to ∞ and 0, respectively, and β and p are constant values. At an intermediate shear rate, the Cross model behaves like a Power-law model. However, unlike the Power-law, the Cross model produces Newtonian μ_0 , μ_{∞} at both very low and high shear rates.

For the GPL model, the constitutive equation, as a function of strain is given by the expression:

$$\begin{cases} \tau = \lambda(\dot{\gamma}) |\dot{\gamma}|^{n(\dot{\gamma})} \\ \mu(\dot{\gamma}) = \lambda(\dot{\gamma}) |\dot{\gamma}|^{n(\dot{\gamma})-1} \end{cases} \quad (6)$$

where λ is the consistency parameter and n is the Power-law exponent given by:

$$\lambda(\dot{\gamma}) = \mu_{\infty} + \Delta\mu \exp \left[- \left(1 + \frac{|\dot{\gamma}|}{a} \right) \exp \left(- \frac{b}{|\dot{\gamma}|} \right) \right]$$

$$n(\dot{\gamma}) = n_{\infty} - \Delta n \exp \left[- \left(1 + \frac{|\dot{\gamma}|}{c} \right) \exp \left(- \frac{d}{|\dot{\gamma}|} \right) \right]$$

where μ_{∞} is the limiting Newtonian viscosity, a , b , c , d , $\Delta\mu$, Δn , and n_{∞} are constant values.

The GPL model is a developed form of the known Power-law, which is modified to account for various factors that would influence blood flow characteristic. It also encapsulates the behaviors of many of the other blood models. Specifically, it behaves Newtonian at high strain rates and has Casson and Carreau models as special cases. Parameters involved in the Cross and GPL models are computed using a non-linear least-squares fitting to experimental data of blood viscosity measured at certain shear rates. In the present work we use viscosity data obtained by Brooks *et al.* [22], for normal human blood at 25 °C, and for an hematocrit of 48%. The Vigne [23] algorithm is used here to fit our models to experimental data. More specially, for each viscosity model of the form $\mu(p, \dot{\gamma}_i)$, we computed the parameters p solution of the minimizing sum of squares errors between the measured data and model's predictions:

$$e(p) = \sum_{i=1}^n [\mu(p, \dot{\gamma}_i) - \mu_{mes}(\dot{\gamma}_i)]^2$$

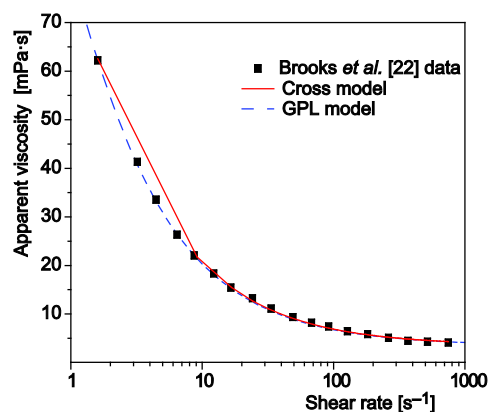


Figure 1. Apparent viscosity vs. shear rate for Cross and GPL models; measured and predicted values

experimental data and theoretical models, shows the highest value and therefore the best fit, for the GPL (0.99) compared to the Cross model (0.87).

For the sake of simplicity, it is assumed that the geometry of the stenosis artery is axisymmetric. Although, the vascular wall is considered as a rigid tube. Geometry of the

where p is the set of admissible parameters. This algorithm involves choosing initial values for the parameters. Then, the parameters are refined iteratively. The fitting of the Cross and GPL models results in the parameters reported in tab. 1. Whereas, fig. 1 shows the curve-fitting result for Cross and GPL models, respectively, it represents the variation of the apparent viscosity with shear rate, and illustrates the comparison between theoretical (solid lines), and measurements data (symbols).

From this figure, both models give a good fit at high shear rate. However, the Cross model present quite different to experimental data regarding the low shear viscosity. The Pearson coefficient (R) which gives the correlation between

Table 1. Cross and GPL models parameters

Parameters and values									
Cross	μ_{∞} , [mPa·s]		μ_0 , [mPa·s]		β , [s]		p		R
	5.24		103.1		1.15		1.25		0.87
GPL	μ_{∞} , [mPa·s]	n_{∞} , [mPa·s]	$\Delta\mu$, [mPa·s]	Δn , [mPa·s]	a	b	c	d	R
	4.59	1.03	140	0.1	1.57	0.32	45	1.82	0.99

artery in the presence of stenosis is constructed mathematically in cosine shaped model (fig. 2) suggested by Young [24]:

$$\frac{r(z)}{D} = 2 \left\{ 1 - \frac{\delta}{D} \left[1 + \cos \frac{\pi(z - z_0)}{L} \right] \right\} \quad (7)$$

Here, L is the width of stenosis, δ the maximum width, and D is the vessel diameter, z_0 is the centre position of stenosis region, fig. 2. In this work, we used a degree of stenosis severity of 75% ($D = 2.0$, $\delta = 0.5$, $L = 2$, $z_0 = 16$). The boundary conditions required to solve the governing equations are:

- The pulsatile flow was generated by means of axial velocity inlet profile imposed as function of the time. This physiological profile contains some periods of reverse flow as well as a maximum inflow velocity of 0.47 m/s with a heart rate of approximately 60 beats per minute (fig. 3).
- The radial velocity is set to zero at the inlet.
- At the outlet of the artery, the fully developed flow condition is applied, we arbitrarily prescribed a zero pressure.
- On all rigid walls, all velocity components were set to zero according to the no-slip condition.
- In the axis of symmetry, both the normal velocity and the first-order derivative of the axial velocity in the radial direction are set to be zero.

Blood was meddled as a Newtonian fluid with a constant dynamic viscosity $\mu_{\infty N}$ of 0.0035 Pa·s, and a density ρ of 1050 kg/m³. This corresponded of $Re = 282$, and Womersley number equal to 2.74.

The governing equations are extremely non-linear and have to be solved numericaly. In this study, the momentum and continuity equations are solved using a finite element code, originally developed by the authors and written in the FORTRAN programming language [25, 26]. The penalty function approach is introduced to eliminate the pressure from the momentum equations, and treat the incompressibility. In this method the continuity equation is replaced by:

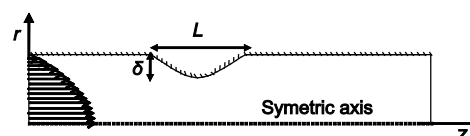


Figure 2. Flow geometry of blood vessels

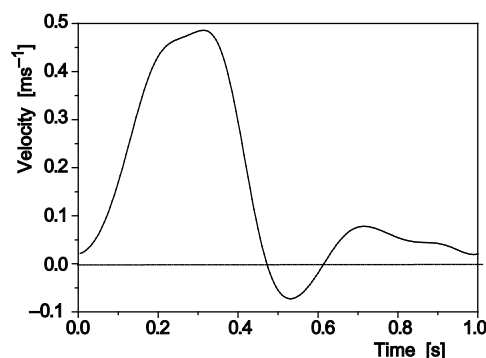


Figure 3. Physiological waveform of inlet velocity

$$p = -\lambda_p \nabla v \quad (8)$$

with penalty parameter λ_p which is assumed to be very large (10^6). So we first solve the velocity from eqs. (2) and (3) and afterwards compute the pressure directly from eq. (8). The discretization of motion eqs. (2) and (3) follows the standard Galerkin formalism. Thus, after assembly, the final equations can be written for each element in a matrix form:

$$\rho[M]\{\dot{v}\} + \rho[N]\{\bar{v}\} - \lambda[P]\{\bar{v}\} + \mu(\dot{\gamma})[S]\{\bar{v}\} = \{\bar{F}\} \quad (9)$$

where [M], [N], [P], and [S] are the mass, convective, penalty, and diffusion matrices, respectively, $\{\dot{v}\}$ – the time derivative of velocity, $\{\bar{v}\}$ – the velocity vector, and $\{\bar{F}\}$ – the force vector.

The non-linear terms in eq. (9), resulting from the advection in the inertial term and the non-Newtonian viscosity behaviour in the constitutive relationship, are solved at each time step over a cardiac pulsation using the Newton iterative technique. The time integration is performed by an implicit first-order time step scheme. The time step is chosen small enough that the stability conditions on the convective and diffusive terms are preserved.

Numerical results and discussion

In order to assess the accuracy of the finite element methods employed, computation for which the analytic solution is well known was performed in pulsatile flow. We test the Womersley solution for an unsteady inlet velocity at mid length of a straight tube where flow is fully developed. The Womersley velocity profile for the axial component of velocity is given by [27]:

$$w(r, t) = \frac{AR^2}{i\mu\alpha^2} \left[1 - \frac{J_0(i^{3/2}\alpha r)}{J_0(i^{3/2}\alpha R)} \right] e^{i\omega t} \quad (10)$$

where J_0 is the first order Bessel function, ω – the angular frequency, A – the amplitude of pulsation, R – the radial distance, and α – the Womersley number. Figure 4 illustrates the numerically computed axial velocities against the analytical solution at five different times of the cardiac cycle. We found a good agreement of the numerical with the analytical results, and a maximum error of less than 0.06%. Further improvements can be made by adopting a much finer mesh.

The computational domain extends from $z = 0$ mm to $z = 46$ mm, in order to have a sufficient development length in the axial direction. Moreover, we run simulation comparisons of blood as a Newtonian fluid by assigning the viscosity $\mu_{\infty N}$ to the blood. Motion equations will be integrated in time for as many cycles as are needed to reach a periodic solution. Typically, five cycles were sufficient to satisfy this condition in our calculations. With these assumptions, numerical results concerning the flow characteristics are presented for streamlines, flow velocities and wall shear stress.

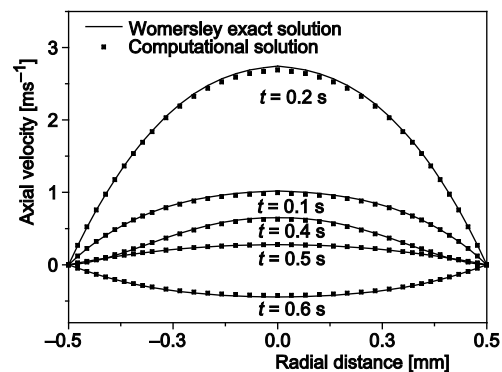


Figure 4. Theoretical and computed axial velocities at five different times

A streamline is the locus of points that are everywhere tangent to the instantaneous velocity vector, *i. e.*, the flow occurs along the directions of the streamlines. The velocity components are related to the stream function:

$$w = -\frac{1}{r} \frac{\partial \psi}{\partial r}, \quad u = \frac{1}{r} \frac{\partial \psi}{\partial z} \quad (11)$$

For a given velocity field, an efficient approach to computing the stream function distribution is based on using the vorticity function defined:

$$\zeta = \frac{\partial u}{\partial r} - \frac{\partial w}{\partial z} \quad (12)$$

By substituting (11) into (12), the following Poisson equation is obtained:

$$\nabla^2 \psi = -\zeta \quad (13)$$

This equation can be easily solved by the finite element method as, using a constant boundary condition at the wall, evaluated by the mass flux entering the tube, and the arbitrary constant of the stream function at the centreline [25].

Figures 5(a) and (b) show the streamlines comparisons of Newtonian and non-Newtonian GPL models blood at various time levels over one pulsatile cycle for stenosis severity of 75%. It is interesting to note that there is a permanent flow separation zone (vortex) formed into the artery, near the wall, for most of the cardiac cycle cases, for both Newtonian and non-Newtonian cases, although, its size and location change during the pulse cycle. These vortex-

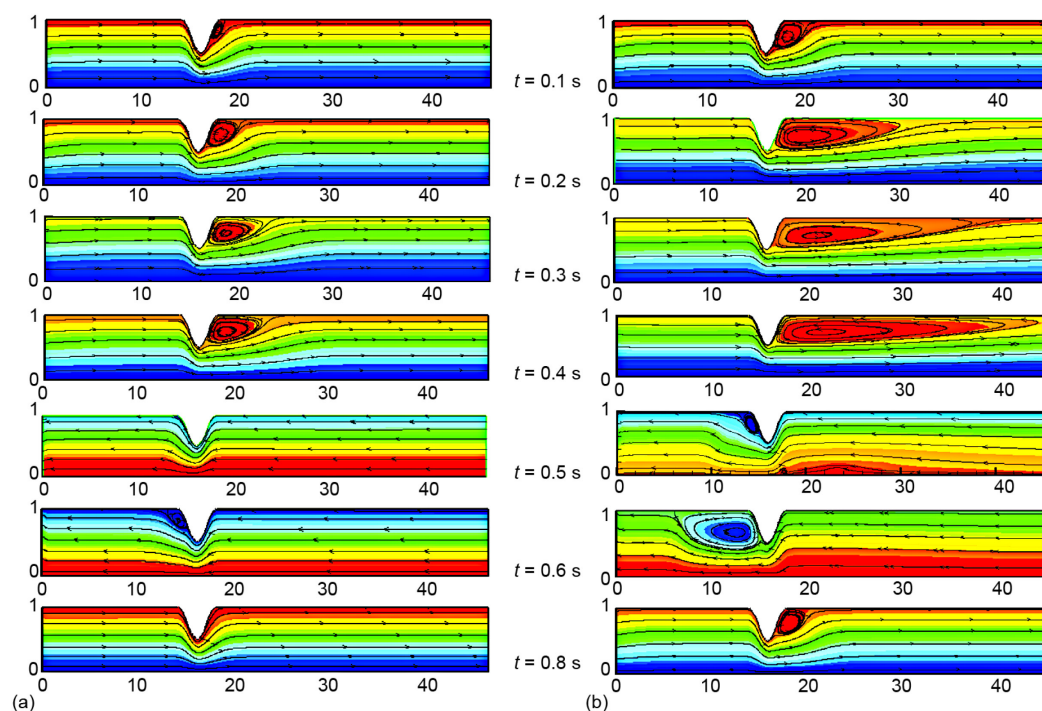


Figure 5. Instantaneous streamlines during a cycle of pulsatile flow; (a) GPL case, (b) Newtonian case
 (for color image see journal web-site)

es are indicative of regions where the flow is reversed over a significant portion of each cycle. Thus, appearance of these separation regions are of pathological significance since, they increase the residence time of blood constituents that could cause the blood clot or thrombosis. During the systolic phase, as the velocity inlet accelerates, the vortex appears downstream of the stenosis throat. Furthermore, as time goes, the vortex becomes bigger. It continues to grow even after the flow decelerates at $t = 0.4$ second. During the diastolic phase as the velocity reaches its negative value at $t = 0.5$ second, the flow reverses direction, and the vortex develops upstream of the stenosis. However, the size of these vortices and their associated separation and reattachment point's locations differ for Newtonian and non-Newtonian models. The Newtonian model provides the largest vortex and the GPL model, fig. 5(a), gives the smallest size vortex and a less disturbed pattern flow than its counterpart. This is acceptable in light of the fact that the GPL model has the largest viscosity in all shear rate ranges and the Newtonian model has the least.

To give an idea of the velocity profiles, using the three different models described previously, we have plotted in figs. 6(a)-(c), the axial flow velocity on the z -axis at three times levels of the pulse period; $t = 0.1$ second (systolic acceleration), $t = 0.3$ second (peak systolic), and $t = 0.6$ second (minimum diastolic phase), for various cross sections of artery. These figures clearly show similarities between the three models at the inflow and outflow (far from the constriction) of the artery, with a developed (parabolic) profile, in which the Newtonian velocity curve overlaps the Cross and GPL curves. While the difference in axial velocity profiles is pronounced at and around the stenosis, with some departures from the parabolic profile, (for $t = 0.1$ and 0.3 second), due to the greater shear force acting on the fluid in these regions. The velocity profile obtained for Newtonian case is relatively flat with uniform velocity in the artery centre and a very steep velocity gradient near the wall. A slightly flattened velocity profile is observed for GPL and Cross models in the centre of artery due to the of the artery. At diastolic phase ($t = 0.6$ second) the flow change direction, and the differences between Newtonian and non-Newtonian cases are maintained for most section of artery, and are shear-thinning behaviour of the fluid viscosity. It implies that, the flow is quicker than the

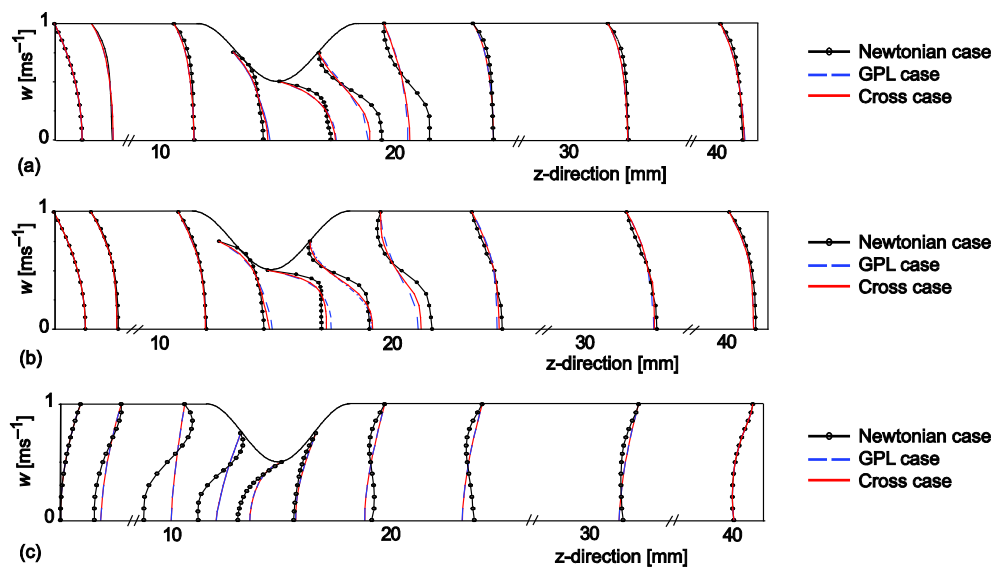


Figure 6. Axial flow velocity profiles on z -axis at: (a) $t = 0.1$ s, (b) $t = 0.3$ s, (c) $t = 0.6$ s

non-Newtonian ones and its patterns remain in a disturbed state over a long distance more pronounced distal to the stenosis. We can also observe that, the differences in velocity profiles are small between Cross and GPL models near the stenosis constriction, and insignificant far from stenosis.

We represent in figs. 7(a)-(c), a comparison of the axial velocity profiles along the symmetric axis, for the three models of blood viscosity in the same flow condition as previous, and at the three times of the period cycle ($t = 0.1$ s, $t = 0.3$ s, $t = 0.6$ s). The maximum velocity in a cycle occurs at the throat of stenosis. As the fluid moves further downstream, the velocity profile becomes stabilized, *i. e.* fully developed flow. Moreover, in fig. 7(c) that the axial velocities predicted by the three models, are negative along the symmetric axis, indicating a complete flow reversal at minimum diastolic time ($t = 0.6$ s). Predictions of axial velocity, for the Newtonian and non-Newtonian blood models differ in regions with high velocity; in stenotic segment and in its neighbourhood. From this plot we observe that during the acceleration phase at low inlet velocity ($t = 0.1$ s) a little practical difference occurred in velocity profile between the three models with the increase of inlet velocity, at $t = 0.3$ s. The peak value of velocity in Newtonian case is much smaller than in non-Newtonian case. Therefore the Newtonian model takes longer for the flow to recover from its disturbed states. This is predictable because of higher viscosity of (than Newtonian viscosity) the non-Newtonian case. Comparison between the two non-Newtonian models shows that treating blood as a GPL or Cross model, led to similar results, as it can be seen in figs. 7(a)-(c), at low inlet velocity ($t = 0.1$ and 0.6 second). While, at $t = 0.3$ s, fig. 7(b), when the inlet velocity is maximal, the difference between the two blood viscosity models appears more significant.

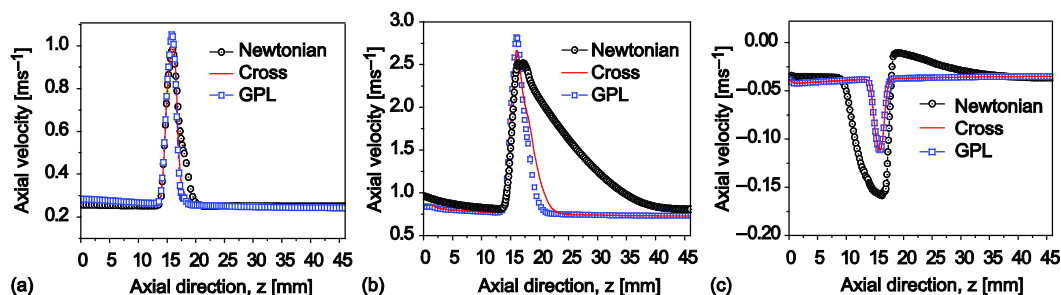


Figure 7. Axial velocity profiles on symmetric axis at: (a) $t = 0.1$ s, (b) $t = 0.3$ s, (c) $t = 0.6$ s, for Newtonian, Cross, and GPL models

The variation of the axial velocity profiles along the radial direction at different times through the cardiac cycle; 0.1 s, 0.3 s, and 0.6 s, are exhibited in figs. 8(a)-(c), respectively. These figures compare and quantify the effects of shear-thinning models of the Cross and the GPL with Newtonian rheology blood at the site of maximum constriction. This result has already been described previously at different cross sections, to show the impact of varying viscosity on flow pattern along the artery. These figures once again, indicate that higher mean velocity is predicted by Newtonian model which exhibits a flat velocity profile, with large central region of uniform reduced velocity during the accelerating phase of systole ($t = 0.1$ s and $t = 0.3$ s). While, for the two non-Newtonian models, the velocity profile is parabolic for $t = 0.1$ s and $t = 0.6$ s, *i. e.* at low inlet velocity, and almost parabolic for $t = 0.3$ s. As it can be seen from fig. 8(b), at $t = 0.3$ s, when the inlet velocity has its maximum value, the Cross and GPL models show a considerable difference, whereas by decreasing inlet velocity ($t = 0.1$ s and $t = 0.6$ s) the difference is hardly recognizable.

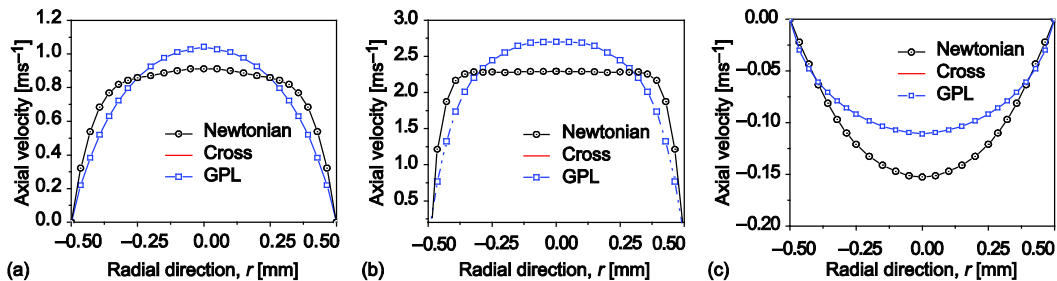


Figure 8. Variation of axial velocity with radial distance at: (a) $t = 0.1$ s, (b) $t = 0.3$ s, (c) $t = 0.6$ s, for Newtonian, Cross, and GPL models

Another hemodynamic interest is the effect of the blood flow behaviour on the wall shear stress as it is believed that wall shear stress is a significant factor in the onset of arterial diseases. Figures 9(a)-(c) show the variation of the shear stress along the wall of stenotic artery at three different times of cardiac cycles, for the different blood viscosity models. The maximum shear stress occurs in the stenotic segment of artery due to the high velocity jet and skewed axial velocity profile. This is followed by an abrupt decrease after the throat region. It becomes negative subsequently, improving a separation zone and a slowdown of the blood in this region. In areas of low shear stress, the luminal surface lipid concentration may be elevated, leading to a greater lipid infiltration, and the onset of atherosclerosis. During early flow acceleration, at $t = 0.1$ s, the wall shear stress curves appear slightly different for the Newtonian and non-Newtonian models. In addition, the curves corresponding to Cross and GPL rheological models are very close, suggesting that the influence of shear thinning on wall shear stress becomes negligible at this time, fig. 9(a). As the flow accelerates at $t = 0.3$ s, fig. 9(b), differences between the three blood viscosity models become noticeable, particularly in the high and low-shear regions; in throat and downstream of stenosis. The Newtonian case gives the highest wall shear stress. In diastolic phase, at $t = 0.6$ s, the magnitude of the reverse flow is not particularly large and so the wall shear stress is uniformly lower the entire artery. An elevated shear stress appeared for the Newtonian blood viscosity. The Cross model deviates slightly from that of GPL in the vicinity of the stenosis throat. Whereas, further from this location, the three curves of wall shear stress are very close suggesting that the influence of the rheological blood behaviour becomes negligible.

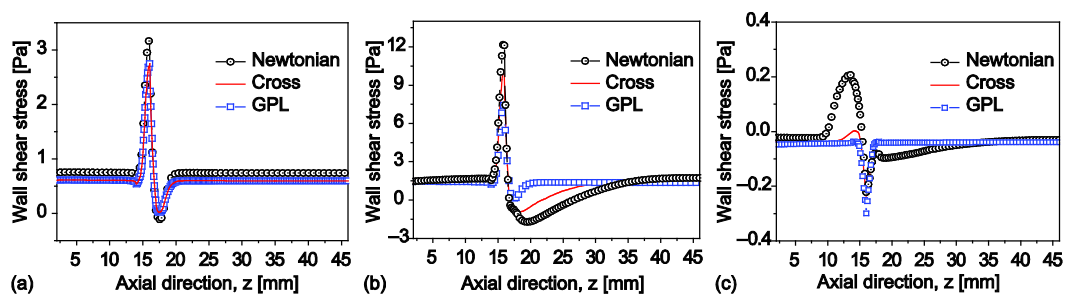


Figure 9. Variation of shear stress along the wall for various times at: (a) $t = 0.1$ s, (b) $t = 0.3$ s, (c) $t = 0.6$ s, for Newtonian, Cross, and GPL models

Conclusions

The pulsatile flow of blood in stenosis artery is simulated by finite element method. Two constitutive laws (Cross and GPL), have been proposed to describe the non-Newtonian

shear-thinning blood viscosity. Both the constitutive models were found to be suitable for describing the non-Newtonian blood viscosity. However, the GPL model provides the best fit and interprets well the blood viscosity at low shear rate. From simulation of pulsatile blood flow through stenotic artery it would be concluded, that using a non-Newtonian model for blood viscosity is an adequate approximation for transient flow over the whole cardiac cycle. The GPL non-Newtonian model provides the less disturbed flow through the stenosis artery compared to both Cross and Newtonian models.

Nomenclature

D – artery diameter, [m]
 p – pressure, [Pa]
 r – radial co-ordinate, [m]
 t – time, [s]
 u – velocity in the r-direction, [m^2s^{-1}]
 z – axial co-ordinate, [m]
 w – velocity in the z-direction, [m^2s^{-1}]

Greek symbols

λ_p – penalty parameter, [-]
 δ – maximum stenosis thickness, [m]
 $\mu_{\infty N}$ – limiting Newtonian viscosity, [Pa·s]
 $\dot{\gamma}$ – shear rate, [s^{-1}]
 ρ – fluid density, [kgm^{-3}]
 τ – shear stress, [Pa]

References

- [1] Lee, J. S., Fung, Y. C., Flow in Locally Constricted Tubes at Low Reynolds Numbers, *Journal of Applied Mechanical*, 37 (1970), 1, pp. 9-16
- [2] Deshpande, M. D., *et al.*, Steady Laminar Flow through Modelled Vascular Stenosis, *Journal of Biomechanics*, 9 (1976), 4, pp. 165-174
- [3] Liepsch, D., *et al.*, Experimental Analysis of the Influence of Stenotic Geometry on Steady Flow, *Biorheology*, 29 (1992), 4, pp. 419-431
- [4] Huang, H., *et al.*, Fluid Mechanics of Stenosed Arteries, *International Journal of Engineering Science*, 33 (1995), 6, pp. 815-828
- [5] Despotisa, G. K., Tsangaris, S., A Fractional Step Method for Unsteady Incompressible Flows on Unstructured Meshes, *International Jou. of Compu. Fluid Dynamics*, 8 (1997), 1, pp. 11-29
- [6] Bertolotti, C., Deplano, V., Three-Dimensional Numerical Simulations of Flow through a Stenosed Coronary Bypass, *Journal of Biomechanics*, 33 (2000), 8, pp. 1011-1022
- [7] Berger, S., Jou, L., Flows in Stenotic Vessels, *Annual Review of Fluid Mechanics*, 32 (2000), Jan., pp. 347-382
- [8] Rodkiewicz, C. M., *et al.*, On the Application of a Constitutive Equation for Whole Human Blood, *Transactions of the ASME, Journal of Biomechanical Engineering*, 112 (1990), 2, pp. 198-206
- [9] Gambaruto, A. M., *et al.*, Sensitivity of Hemodynamics in a Patient Specific Cerebral Aneurysm to Vascular Geometry and Blood Rheology, *Mathematical Biosciences and Engineering*, 8 (2011), 2, pp. 409-423
- [10] Achab, L., Benhadid, S., Application of a Constitutive Law in the Digital Study of Blood Flow through a Stenotic Artery (in French), *Rheologie*, 7 (2005), pp. 28-34
- [11] Sankar, D. S., A Two-Fluid Models for Pulsatile Flow in Catheterized Blood Vessels, *International Journal of Non-Linear Mechanics*, 44 (2009), 4, pp. 337-351
- [12] Chakravarty, S., Datta, A., Pulsatile Blood Flow in a Porous Stenotic Artery, *Mathematical and Computer Modelling*, 16 (1992), 2, pp. 35-54
- [13] Jung, H., *et al.*, Asymmetric Flows of Non-Newtonian Fluids in Symmetric Stenosed Artery, *Korea-Australia Rheology Journal*, 16 (2004), 2, pp. 101-108
- [14] Goubergrits, L., *et al.*, Impact and Choice of a Non-Newtonian Blood Model for Wall Shear Stress Profiling of Coronary Arteries, *Proceedings, 14th Biomedical Engineering and Medical Physics Conf.*, Riga, Latvian, 2008, Vol. 20, pp. 111-114
- [15] Akbar, N. S., *et al.*, Influence of Mixed Convection on Blood Flow of Jeffrey Fluid through a Tapered Stenosed Artery, *Thermal Science*, 17 (2013), 2, pp. 533-546
- [16] Neofytou, P., Comparison of Blood Rheological Models for Physiological Flow Simulation, *Biorheology*, 41 (2004), 6, pp. 693-714
- [17] Tu, C., Deville, M., Pulsatile Flow of Non-Newtonian Fluids through Arterial Stenoses, *Journal of Biomechanics*, 29 (1996), 7, pp. 899-908

- [18] Buchanan, J. R., et al., Rheological Effects on Pulsatile Hemodynamics in a Stenosed Tube, *Computers and Fluids*, 29 (2000), 6, pp. 695-724
- [19] Modarres Razavi, M. R., et al., Numerical Study of Hemodynamic Wall Parameters on Pulsatile Flow through Arterial Stenosis, *IUST International Journal of Engineering Science*, 17 (2006), 3-4, pp. 37-46
- [20] Ballyk, P. D., et al., Simulation of Non-Newtonian Blood Flow in an End-to-End Anastomosis, *Biorheology*, 31 (1994), 5, pp. 565-586
- [21] Cross, M. M., Rheology of Non Newtonian Fluids: A New Flow Equation for Pseudoplastic Systems, *Jou. Colloid Sci.*, 20 (1965), 5, pp. 417-437
- [22] Brooks, D. E., et al., Interactions Among Erythrocytes under Shear, *J. Appl. Physiol.*, 28 (1970), 2, pp. 172-177
- [23] Vigne, J., *Analysis and Use of Numerical Algorithms. Non-Linear Equations and Systems, Vol. 2* (in French), Technip, Paris, 1980
- [24] Young, D. F, Tsai, F. Y., Flow Characteristics in Models of Arterial Stenosis-I Steady Flow, *Journal of Biomechanic*, 6 (1973), 4, pp. 395-410
- [25] Zienkiewicz, O. C., Taylor, R. L., *The Finite Element Method, Vol.3, Fluid Dynamics*, Butterworth-Heinemann, Oxford, UK, 2000
- [26] Dhatt, G., et al., *Methode des Elements Finis (Finite Element Method, in French)*, Hermes, Lavoisier, France, 2005
- [27] Womersley, J. R, Method for the Calculation of Velocity, Rate of Flow and Viscous Drag in Arteries When the Pressure Gradient is Known, *Journal of Physiology*, 127, (1955), 3, pp. 553-563